Am J Physiol Renal Physiol 327: F314–F326, 2024.
First published June 27, 2024; doi:10.1152/ajprenal.00039.2024

american physiological society

AMERICAN JOURNAL OF PHYSIOLOGY
RENAL PHYSIOLOGY

RESEARCH ARTICLE

Perinatal asphyxia leads to acute kidney damage and increased renal susceptibility in adulthood

Tamas Lakat,[1,2]* Andrea Fekete,[1,2]* Kornel Demeter,[3] Akos R. Toth,[1,2] Zoltan K. Varga,[4] Attila Patonai,[5] Hanga Kelemen,[4] Andras Budai,[6] Miklos Szabo,[2] Attila J. Szabo,[2] Kai Kaila,[7] Adam Denes,[8] Eva Mikics,[4]* and Adam Hosszu[1,2]*

[1]*MTA-SE Lendület "Momentum" Diabetes Research Group, Budapest, Hungary;* [2]*Pediatric Center, Semmelweis University, Budapest, Hungary;* [3]*Behavioral Studies Unit, HUN-REN Institute of Experimental Medicine, Budapest, Hungary;* [4]*Translational Behavioral Neuroscience Research Group, HUN-REN Institute of Experimental Medicine, Budapest, Hungary;* [5]*Department of Surgery, Transplantation and Gastroenterology, Semmelweis University, Budapest, Hungary;* [6]*Department of Pathology, Forensic and Insurance Medicine, Semmelweis University, Budapest, Hungary;* [7]*Molecular and Integrative Biosciences Research Programme, Neuroscience Center (HiLIFE), University of Helsinki, Helsinki, Finland; and* [8]*Laboratory of Neuroimmunology, HUN-REN Institute of Experimental Medicine, Budapest, Hungary*

Abstract

Perinatal asphyxia (PA) poses a significant threat to multiple organs, particularly the kidneys. Diagnosing PA-associated kidney injury remains challenging, and treatment options are inadequate. Furthermore, there is a lack of long-term follow-up data regarding the renal implications of PA. In this study, 7-day-old male Wistar rats were exposed to PA using a gas mixture (4% O_2; 20% CO_2 in N_2 for 15 min) to investigate molecular pathways linked to renal tubular damage, hypoxia, angiogenesis, heat shock response, inflammation, and fibrosis in the kidney. In a second experiment, adult rats with a history of PA were subjected to moderate renal ischemia-reperfusion (IR) injury to test the hypothesis that PA exacerbates renal susceptibility. Our results revealed an increased gene expression of renal injury markers (kidney injury molecule-1 and neutrophil gelatinase-associated lipocalin), hypoxic and heat shock factors (hypoxia-inducible factor-1α, heat shock factor-1, and heat shock protein-27), proinflammatory cytokines (interleukin-1β, interleukin-6, tumor necrosis factor-α, and monocyte chemoattractant protein-1), and fibrotic markers (transforming growth factor-β, connective tissue growth factor, and fibronectin) promptly after PA. Moreover, a machine learning model was identified through random forest analysis, demonstrating an impressive classification accuracy (95.5%) for PA. Post-PA rats showed exacerbated functional decline and tubular injury and more intense hypoxic, heat shock, proinflammatory, and profibrotic response after renal IR injury compared with controls. In conclusion, PA leads to subclinical kidney injury, which may increase the susceptibility to subsequent renal damage later in life. In addition, the parameters identified through random forest analysis provide a robust foundation for future biomarker research in the context of PA.

NEW & NOTEWORTHY This article demonstrates that perinatal asphyxia leads to subclinical kidney injury that permanently increases renal susceptibility to subsequent ischemic injury. We identified major molecular pathways involved in perinatal asphyxia-induced renal complications, highlighting potential targets of therapeutic approaches. In addition, random forest analysis revealed a model that classifies perinatal asphyxia with 95.5% accuracy that may provide a strong foundation for further biomarker research. These findings underscore the importance of multiorgan follow-up for perinatal asphyxia-affected patients.

kidney injury; perinatal asphyxia; random forest; renal biomarkers

INTRODUCTION

Perinatal asphyxia (PA) is a significant cause of mortality, leading to 900,000 neonatal deaths worldwide (1). In the much larger number of survivors, PA is a predominant etiological factor of lifelong neurodevelopmental disabilities including cerebral palsy, attention deficit disorders, and cognitive dysfunction (2, 3). Selective head or whole body cooling is the current gold standard treatment that reduces mortality and improves neurological outcomes, but almost half of the affected neonates still suffer from developmental disabilities (4, 5). Clinical guidelines mainly concentrate on long-term follow-up of cognitive conditions. Data are scarce on the possible permanent deterioration of peripheral organs following PA, which hampers the development of therapies targeting more general underlying mechanisms and alleviating its multiple pathophysiological consequences (6).

Although the central nervous system is the most vulnerable organ system to asphyxic events, multiorgan dysfunction—particularly kidney injury—has also been demonstrated in

*T. Lakat and A. Fekete contributed equally to this work; E. Mikics and A. Hosszu contributed equally to this work.
Correspondence: A. Hosszu (hosszu.adam@semmelweis.hu).
Submitted 6 February 2024 / Revised 23 May 2024 / Accepted 17 June 2024

clinical studies (5, 7). During the first postnatal days, ~40% of affected neonates develop acute kidney injury (AKI) (5, 6), associated with a mortality rate exceeding 30% and increasing the risk of chronic kidney disease in later life (8). Furthermore, renal complications are bound to have deleterious effects on brain development and functions, worsening the severity of adverse neurological outcomes (7, 9).

The neonatal kidney is highly susceptible to hypoxia. Reduced renal perfusion and subsequent tubular injury leading to renal parenchymal damage develop quickly after birth and can manifest in severe AKI. Furthermore, there is growing evidence that even a subclinical increase in renal retention parameters [serum creatinine (sCr) and blood urea nitrogen (BUN)] provokes a higher risk for chronic kidney disease (CKD) in the long run (10, 11). Early recognition is crucial to mitigate long-term consequences; however, diagnosis is still challenging since appropriate biomarkers are lacking. In addition, undetected injuries often appear in tandem with acute events later in life, such as ischemia-reperfusion (IR) injury or renal decline due to aging, as these will act as a secondary challenge for formerly damaged organs (12). serum

Currently, no treatment prevents asphyxia-induced renal damage; thus, preclinical research should aim at identifying disease mechanisms and developing novel therapeutic approaches. Here we investigated renal impairment following PA and identified the main pathways involved, including hypoxic and heat shock response, inflammation, and profibrotic routes. We hypothesized that postasphyxic kidney damage has long-term consequences leading to increased renal vulnerability in adulthood. Thus, experiments with moderate bilateral renal ischemia were done on adult rats with a history of PA. We used the random forest algorithm to determine cross correlations between various solid parameters to identify potential novel biomarkers for early diagnosis.

MATERIALS AND METHODS

Animals

All experiments were carried out by the Council on Animal Care of the National Health Institution of Hungary (PEI/001/828-4/2015).

Charles-River Wistar rats (Charles-River Laboratories, Sulzfeld, Germany) from the breeding colony of the HUN-REN Institute of Experimental Medicine (Budapest, Hungary) were used. Rats were kept in groups of three or four in temperature-controlled (24 ± 1°C) and humidity-controlled (rel. 50 ± 10%) rooms under a 12:12-h light/dark cycle. Standard laboratory food and tap water were available ad libitum. Dams were isolated for pregnancy. Litters were standardized to 8–10 pups/litter on the day of birth (*postnatal day 0*) to avoid significant variations in maternal care of pups. Only male pups were enrolled in the experiments. The minimum sample size was chosen to facilitate appropriate statistical analysis. The experimental protocol is summarized in Fig. 1.

Experimental Protocols and Treatment Groups

Experiment I: perinatal asphyxia.

On *postnatal day 7*, pups were separated from the dam and randomly assigned to groups (n = 6–10 animals/group) as follows:

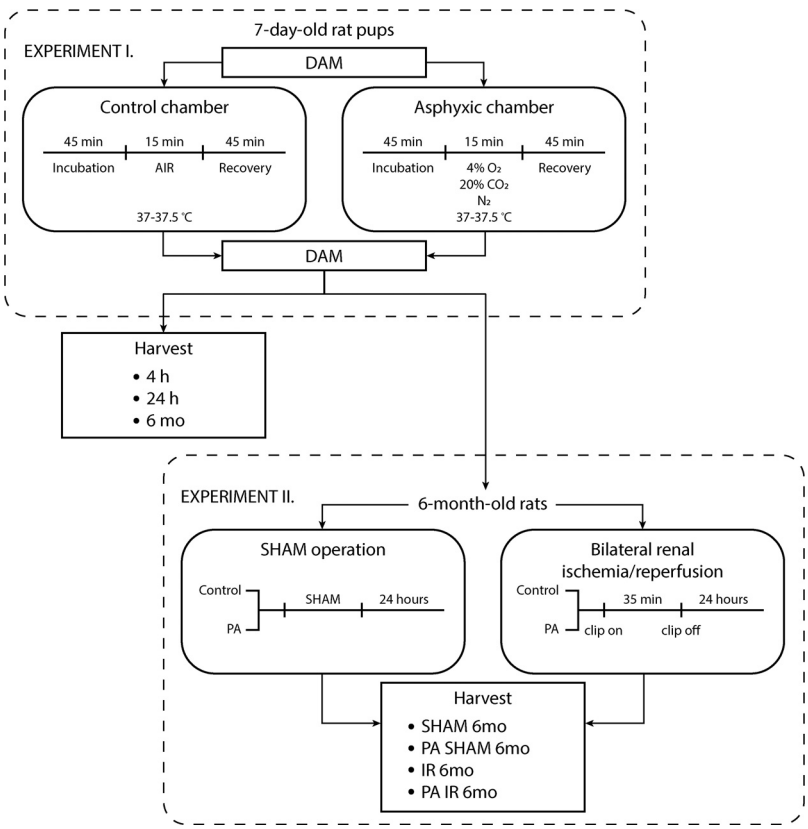

Figure 1. Schematic of perinatal asphyxia (PA) and renal ischemia/reperfusion (IR) rat model.

Control: Pups were placed individually in isothermal control chambers and incubated for 105 min (core body temperature = 37.0°C–37.5°C) and then were returned to the dams.

PA: Instead of pure hypoxia, as used in most published work on PA in rodent models, rats were exposed to a gas mixture containing a low level of oxygen and a high level of CO_2 to better mimic the PA conditions. Notably, recent work on rats has demonstrated marked differences—including qualitative ones—in cardiorespiratory and neurophysiological responses to hypoxia in the presence and absence of elevated CO_2 (13, 14). Here, pups were placed in isothermal treatment chambers and incubated for 45 min to equilibrate core body temperature (37.0°C–37.5°C, monitored by the rectal temperature of a sentinel animal). After 45 min, asphyxic treatment chambers were filled with the asphyxic gas mixture (4% O_2 and 20% CO_2 in N_2). The asphyxic insult was terminated after 15 min and the gas mixture was rapidly replaced with room air. Pups were allowed to recover for 45 min and then were returned to the dams. All treatment chambers were placed on an isothermal (36°C) water bath (WNB 45, Memmert). O_2 and CO_2 concentrations, temperature (25°C–28°C), and humidity (21%–25%) were monitored and recorded (TR250Z Oxygen Sensor, K-33 BLG Sensor, CO2Meter). Animals that died during the insult due to acute apnea, which has no relation to kidney functions, were not included in the experiment. Animals were euthanized by decapitation 4 h, 24 h, or 6 mo after the insult. Blood samples were collected and centrifuged, and sera were immediately snap-frozen. Kidney samples were collected and immediately snap frozen in liquid nitrogen or fixed in 8% buffered paraformaldehyde (pH 7.4) for further investigation.

Experiment II: effect of perinatal asphyxia on renal ischemia-reperfusion injury in adulthood.

Control and PA rats were weaned on *postnatal day 21* and kept in same-age, same-treatment groups of three or four. At 6 mo, rats were randomized into the following groups: SHAM 6 mo, IR 6 mo, and PA IR 6 mo. Moderate renal IR was performed on control (IR 6 mo) and PA-affected (PA IR 6 mo) rats. General anesthesia was induced intraperitoneally by using a ketamine (75 mg/kg) and xylazine (10 mg/kg) mixture. Body temperature was maintained close to 37°C on a heating pad. Bilateral renal ischemia was accomplished by cross-clamping the renal pedicles for 35 min. Sham operated animals (SHAM 6 mo) served as controls. Twenty-four hours after reperfusion, rats were reanesthetized and euthanized by exsanguination. Blood and kidney samples were collected ($n = 6$ or 7 animals/group).

RT-qPCR

Total RNA was extracted from the kidneys using the Total RNA Isolation Mini Kit (Geneaid Biotech, New Taipei City, Taiwan). First strand cDNA was prepared from 2 μg of total RNA using the Maxima First Strand cDNA Synthesis Kit for RT-qPCR (Thermo Fisher Scientific, Waltham, MA). Real-time RT-PCR was performed on the LightCycler 96 system (Roche Diagnostics, Mannheim, Germany). The primers (IDT, Coralville, IA) used in this study are listed in Supplemental Table S1. Results were analyzed and normalized to the expression of the *Rn18s* housekeeping gene from the same samples as the reference transcript.

Renal Histology

Renal tissues were fixed in 8% neutral buffered paraformaldehyde, dehydrated in graded alcohol series, embedded in paraffin, cut to 3-μm-thick sections, and mounted on coated glass microscope slides. Sections were stained with periodic acid-Schiff (PAS), Masson's trichrome, or picrosirius red reagent.

Tubular lumen dilatation was evaluated in a double-blinded fashion, semi-quantitatively on three fields of view/animal of PAS-stained kidney sections (×200 magnification). The average proximal tubular area was quantified using Adobe Photoshop CC 2018 software version 19.1.6 20180808. r.398 (Adobe Systems, San Jose, CA) and ImageJ software version 1.52a (National Institutes of Health, Bethesda, MD; Laboratory for Optical and Computational Instrumentation, University of Wisconsin, Madison, WI).

Immunohistochemistry

Sections were prepared as described earlier. After deparaffinization and rehydration, samples were pretreated with heat-induced epitope retrieval in 1 mM (pH 6.0) citrate buffer for 15 min at 750 W. Tissues were washed in Tris-buffered saline solution (TBS) (pH 7.6) and were incubated in anti-CD68 (Cat. No. MCA341GA, Bio-Rad Laboratories, Hercules, CA; 1:500; 1 h, room temperature), anti-kidney injury molecule (KIM)-1 (Cat. No. AF3689-SP, R&D Systems, Minneapolis, MN; 10 μg/mL; 1 h, room temperature), or anti-neutrophil gelatinase-associated lipocalin (NGAL) (Cat. No. 26991-1-AP, Proteintech Group, Rosemont, IL; 1:200; 1 h, room temperature). Sections were washed in TBS and incubated with the HISTOLS-R anti-rabbit (CD68, NGAL)/anti-goat (KIM-1) HRP-labeled detection system (Cat. No. 30011.R500, Histopathology, Pécs, Hungary; 30 min, room temperature). After washing in TBS, the reaction was developed with the HISTOLS Resistant AEC Chromogen/substrate System (Cat. No. 30015.K, Histopathology). Sections were counterstained with hematoxylin solution.

Immunohistochemical labeling was assessed using H-score (1 × percentage of weak staining) + (2 × percentage of moderate staining) + (3 × percentage of strong staining) on whole slide tissue sections (15).

Statistical Analysis

Results are presented as means ± SD. Statistical analysis was performed using Prism software (GraphPad Prism version 9.4.1, GraphPad Software, San Diego, CA). Statistical tests are summarized in Supplemental Table S2. P values of <0.05 were considered significant. Outlier data points were identified and excluded based on either ROUT or Grubbs' analysis.

Random Forest Classification and Correlation Analysis

The random forest (RF) machine learning algorithm was applied to decrease the dimensions of multivariate data and to identify significant consequences of the

asphyxic insult (16). RF ranks the importance of each variable in the classification of experimental subjects to treatment groups.

To enhance the statistical power of our analysis, samples from all sampling events were used in which complete datasets were available, implying $n = 10$ and 12 samples in the control and PA groups, respectively. In our analysis, *1*) a saturated model using all 20 features was implemented; *2*) these features were ranked according to their importance; *3*) subset models possessing the eight, four, three, and two most relevant variables were created; and *4*) subset models were compared according to group-wise and overall classification accuracy.

All models produced 10,000 decision trees and analyzed four features at a time. Sampling was balanced to 10-10 subjects per group in the RF analysis. Variable importance was ranked based on permutation importance and Gini indices. Spearman correlation analysis was done using Hmisk and qgraph packages (17). Variable selection in RF analysis was done by using RF and VSURF packages (18, 19). All classification methods were done in R statistical environment (20).

RESULTS

Perinatal Asphyxia Leads to Acutely Impaired Renal Function

BUN levels were measured to determine the detrimental effect of PA on renal excretory function. BUN levels increased 4 h (22.41 ± 7.863 mg/dL vs. 34.96 ± 10.99 mg/dL; $P = 0.0162$) after PA, but no difference was detected between the groups at 24 h (Fig. 2*A*). Creatinine levels were undetectable at the age of 7 days.

KIM-1 and NGAL are sufficient biomarkers for AKI in adults and have growing relevance in neonatal AKI prediction (21). Here, renal mRNA expressions of KIM-1 and NGAL (Fig. 2, *B* and *C*) were upregulated in the PA group at 24 h; moreover, KIM-1 was induced as early as 4 h.

AKI caused by ischemic events is typically characterized by progressive tubular damage. Interestingly, PAS-stained kidney tissue sections (Fig. 2*D*) revealed no visible structural changes (epithelial cell death, loss of the brush border, and the subsequent dilation of proximal tubules or cast formation) 24 h following PA. Immunohistochemical labeling demonstrated that KIM-1 protein levels were elevated in the tubules at both time points after PA (Fig. 2*E*). However, NGAL levels showed no significant difference between the groups (Fig. 2*F*).

At the age of 6 mo, BUN (18.4874 ± 1.078 mg/dL vs. 24.46 ± 7.055 mg/dL; $P = 0.2436$) and creatinine clearance (27.69 ± 6.74 mL/min/100 g body wt vs. 21.89 ± 9.18 mL/min/100 g body wt; $P = 0.2406$) levels were not altered significantly in PA-affected rats (Fig. 2*A*). Renal KIM-1 and NGAL (Fig. 2, *B* and *C*) mRNA expression showed no difference from the controls. At this point, morphological changes associated with renal aging (thickened glomerular and tubular basement membrane, hyalinization, and dilation of proximal tubules) developed; however, prior PA did not escalate these changes (Fig. 2*D*).

Perinatal Asphyxia Triggers Angiogenesis and Heat Shock Response via Activating Hypoxic Pathways in the Kidney

Hypoxia inducible factor (HIF)-1α is a crucial transcription factor that regulates an array of genes to maintain cell survival mechanisms under hypoxic conditions (22). Renal HIF-1α mRNA expression (Fig. 3*A*) was elevated rapidly in rats affected by PA and increased further at 24 h. Gene expression of vascular endothelial growth factor A (VEGFA), heat shock factor (HSF)-1, and heat shock protein (HSP)-27 (Fig. 3, *B–F*) downstream elements were also activated at 24 h. Interestingly, significant elevation was detected in the expression of Toll-like receptor (TLR)-2 and HSP-27 at the age of 6 mo.

PA did not affect TLR-4 and HSP-72 expression significantly (Fig. 3*G*).

Perinatal Asphyxia Activates Inflammatory Pathways in the Kidney

Intrarenal inflammation is a primary response to AKI, which involves the production of proinflammatory cytokines and chemoattractants and the recruitment of immune cells to promote repair and regeneration (23).

Four hours after PA, renal expression of monocyte chemoattractant protein (MCP)-1 (Fig. 4*E*) was induced as the first sign of the inflammatory response. In comparison, at 24 h, expression of interleukin (IL)-1β, IL-6, tumor necrosis factor (TNF)-α, and MCP-1 proinflammatory cytokines and chemokines (Fig. 4, *B–E*) were robustly upregulated. Interestingly, no CD68 + macrophage exaggeration was detected following PA (Fig. 4*F*). Increased mRNA expression returned to control levels by the age of 6 mo.

Perinatal Asphyxia Induces Profibrotic Processes in the Kidney

Renal inflammation is associated with increased profibrotic growth factor and extracellular matrix (ECM) component secretion that results in tissue remodeling and fibrotic tissue deposition (24).

Expression of profibrotic growth factors transforming growth factor (TGF)-β and connective tissue growth factor (CTGF) (Fig. 5, *A* and *C*) increased threefold 24 h after PA. Platelet-derived growth factor-β (PDGF-B) gene expression showed tendentious elevation at 4 and 24 h, but this change was statistically not significant. The ECM component fibronectin expression showed significant increase 24 h after PA (Fig. 5*D*).

At the age of 6 mo, there was a modest difference in CTGF (Fig. 5*C*) and fibronectin expression (Fig. 5*D*). Surprisingly, Masson's trichrome and picrosirius red staining (Fig. 5*E*) revealed no ECM component enrichment in post-PA rats.

Perinatal Asphyxia Persistently Increases the Severity of Renal Injury in Adulthood

Since immature kidneys are extremely sensitive to hypoxia, harmful events occurring during the perinatal period may eventuate in long-lasting susceptibility to renal injury. To test our hypothesis, 6-mo-old control (IR group) and post-PA (PA IR group) rats were subjected to moderate renal ischemia. As expected, 24 h after reperfusion, serum levels of renal retention parameters were significantly elevated,

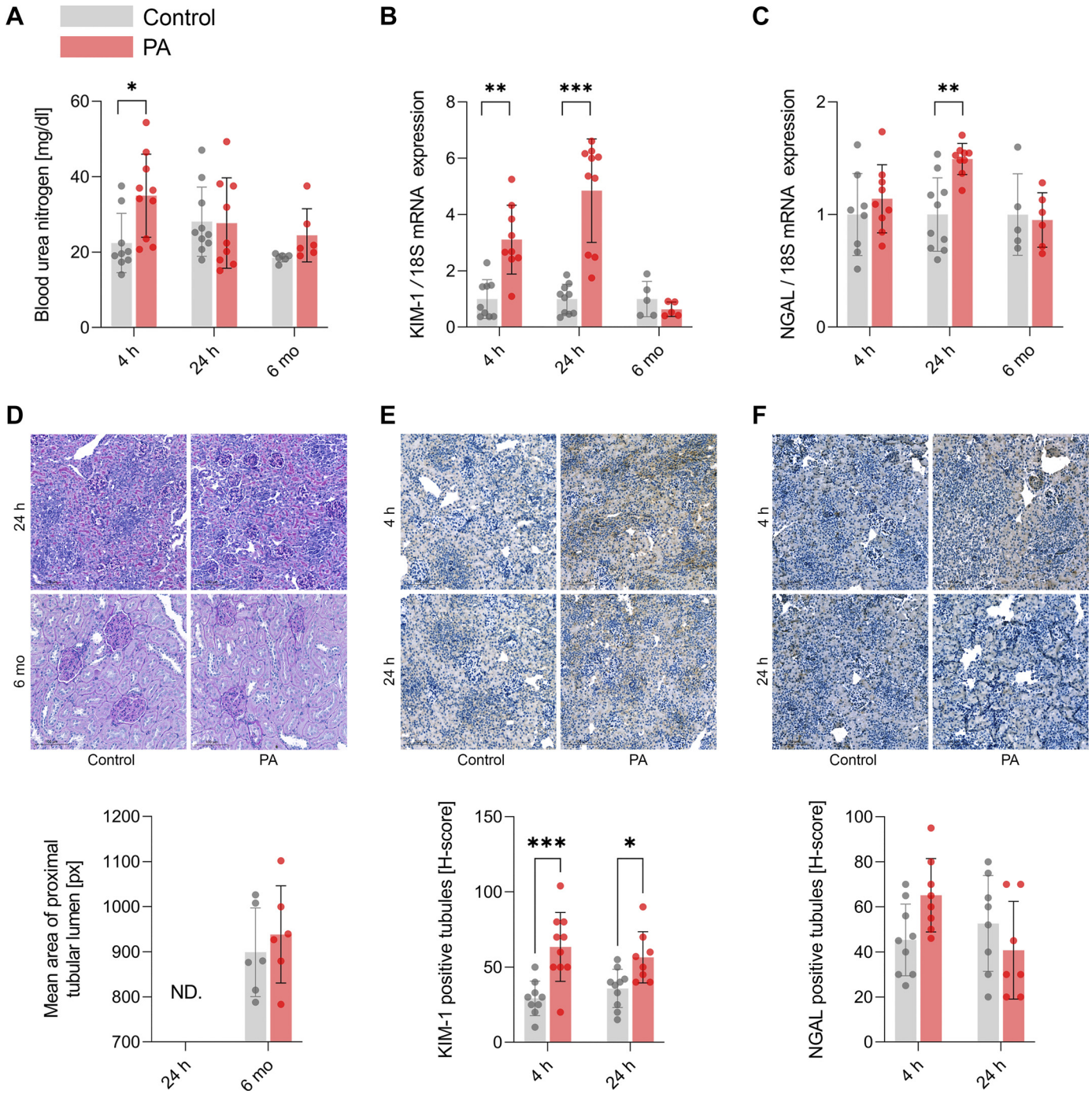

Figure 2. Perinatal asphyxia (PA) impairs renal function and induces acute renal injury. *A*: blood urea nitrogen levels. *B* and *C*: renal mRNA expression of kidney injury molecule-1 (KIM-1; *Havcr1*) (*B*) and neutrophil gelatinase-associated lipocalin (NGAL; *Lcn2*) (*C*). Cycle numbers were normalized to the 18S rRNA (*Rn18s*) housekeeping gene and presented as fold changes compared with controls. *D*: representative images of periodic acid-Schiff-stained kidney tissue sections (scale bar = 100 μm) to assess tubular lumen area (px. indicates pixel number). *E*: immunohistochemical evaluation of anti-KIM-1-labeled kidney tissue sections (scale bar = 100 μm) using H-score. *F*: immunohistochemical evaluation of anti-NGAL-labeled kidney tissue sections (scale bar = 100 μm) using H-score. *P* values were determined by two-way ANOVA followed by Holm–Šídak's multiple-comparison (NGAL) or Kruskal–Wallis test followed by Dunn's multiple comparison (blood urea nitrogen and KIM-1). $*P < 0.05$ vs. control; $**P < 0.01$ and $***P < 0.001$ vs. control. $n = 5$–10/group. Gray bars represent the control group; red bars represent the PA group. Bars indicate means ± SD. ND, not detectable.

production of AKI biomarkers was increased considerably, and typical structural alterations were evident.

More importantly, significantly higher BUN (93.44 ± 25.87 vs. 115.0 ± 12.09 mg/dL; $P = 0.040$) and sCr (2.856 ± 0.9634 vs. 3.853 ± 1.058; $P = 0.046$) levels (Fig. 6*A*) were measured in post-PA rats compared with IR rats 24 h after reperfusion. Correspondingly, renal mRNA expressions of both KIM-1 and NGAL (Fig. 6*D*) were higher in the PA IR versus IR group. Histological evaluation (Fig. 6*B*) revealed no difference in post-ischemic structural changes such as dilation of proximal

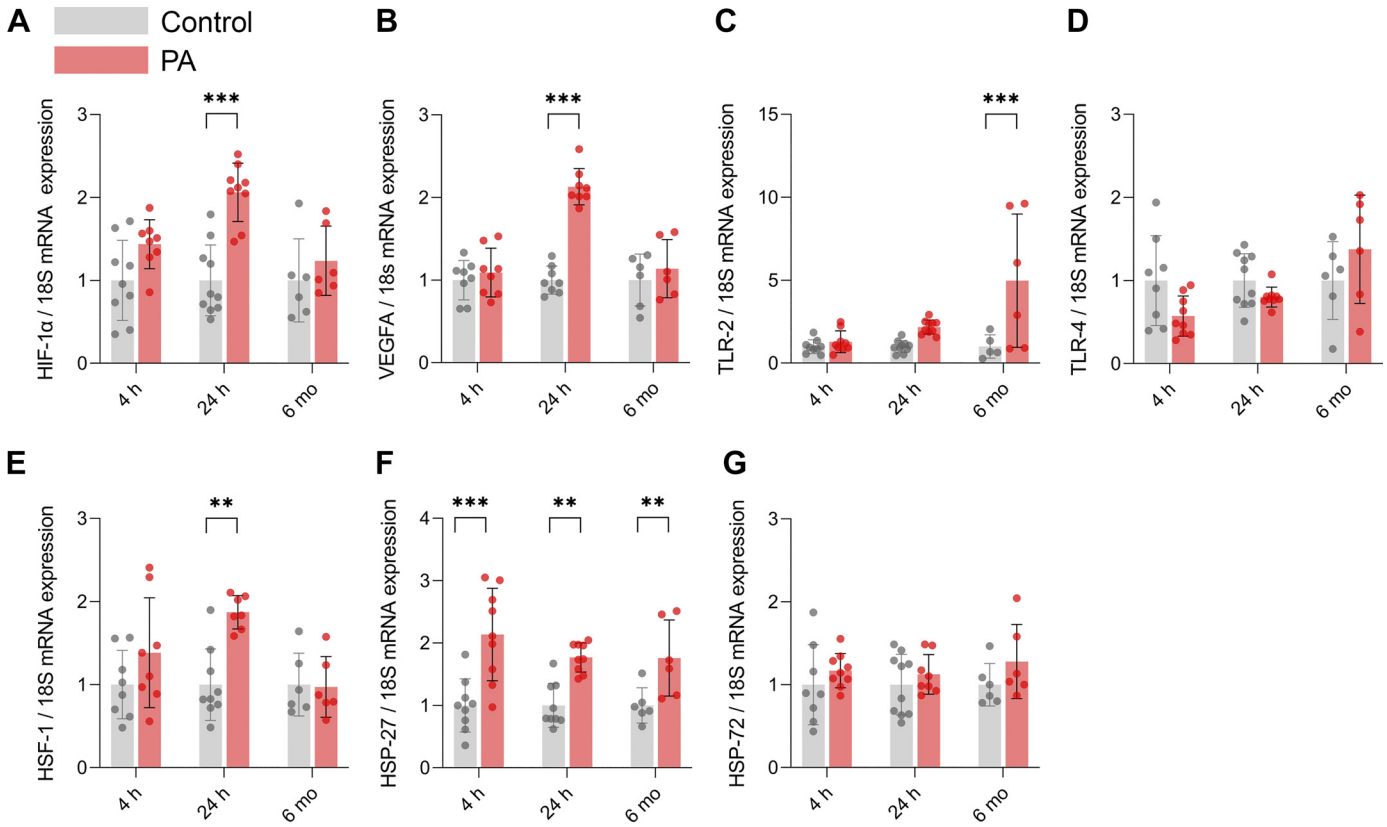

Figure 3. Perinatal asphyxia (PA) upregulates renal hypoxic and angiogenic processes and activates heat shock response. *A–G*: renal mRNA expression of hypoxia-inducible factor (HIF)-1α (*Hif1a*) (*A*), vascular endothelial growth factor A (VEGFA; *Vegfa*) (*B*), Toll-like receptor (TLR)-2 (TLR-2; *Tlr2*) (*C*), TLR-4 (*Tlr4*) (*D*), heat shock factor (HSF)-1 (*Hsf1*) (*E*), heat shock protein (HSP)-27 (*Hspb1*) (*F*), and HSP-72 (*Hspa2*) (*G*). Target gene expression levels were normalized to the 18S rRNA (*Rn18s*) housekeeping gene and presented as fold changes compared with controls. *P* values were determined by two-way ANOVA followed by Holm–Šídak's multiple-comparison (HIF-1α, VEGFA, TLR-2, HSF-1, HSP-27, and HSP-72) or Kruskal–Wallis test followed by Dunn's multiple comparison (TLR-4). $*P < 0.05$, $**P < 0.01$, and $***P < 0.001$ vs. control. $n = 6$–10/group. Gray bars represent the control group; red bars represent the PA group. Bars indicate means ± SD.

tubules [1246 ± 211.2 pixels (px) vs. 1343 ± 77.20 px; $P = 0.49$] or tubular damage (score 3.837 ± 0.4661 vs. 4.054 ± 0.4203; $P = 0.4416$).

IR induced HIF-1α expression only in post-PA rats, whereas activation of the downstream pathway differed from what was observed in pups. PA had no impact onVEGFA and TLR-2 expression levels following IR. Interestingly, TLR-4 expression was significantly lower in the PA IR group compared with the IR group. Similar to HIF-1α, elevations of renal HSF-1 and HSP-72 gene expression levels were higher in the PA IR group versus the IR group (Fig. 6*D*).

Renal mRNA expressions of inflammatory cytokines IL-1β, IL-6, and MCP-1 were significantly elevated in the PA IR group (Fig. 6*D*). Conversely, CD68 labeling (Fig. 6*C*) revealed no macrophage infiltration.

Renal expression of TGF-β increased to the same extent in both the IR and PA IR groups. However, the elevation of PDGF-B and CTGF was about two times higher in post-PA rats. PA had no additional effect on fibronectin levels following IR (Fig. 6*D*).

Machine Learning-Based Screening of the Consequences of Perinatal Asphyxia

PA caused the activation of renal hypoxic, proinflammatory, and profibrotic pathways with a significant elevation of mRNA expression of a wide range of downstream elements (summarized in Supplemental Fig. S1). Furthermore, our results clearly demonstrate that PA has long-term consequences by permanently increasing the sensitivity and severity of renal ischemic damage.

To identify potential novel biomarkers, we aimed to find the fewest parameters that sufficiently describe the physiological consequences of PA. Correlation analysis between control and PA groups (Fig. 7*A*) revealed a shifted association pattern in response to asphyxia.

RF classification was used to highlight the most relevant differences; one saturated (20 variables) and several subset models (8, 4, 3, or 2 variables) were created (Fig. 7*B*). The saturated model classified asphyxia-treated subjects with 100% accuracy and control subjects with 80% accuracy, indicating false-positive treatment identifications. Simpler subset models marginally decreased PA (−8%) but markedly increased control classification accuracy (+20%). The subset model that used the three most essential variables (KIM-1, HSP-27, and HIF-1α) performed best with an overall 95.5% accuracy.

The ranking of variables was similar in permutation- and Gini index-based analysis (Fig. 7*C*). The expression levels of the eight most essential variables showed a significant difference between the control and PA groups (Fig. 7*D*).

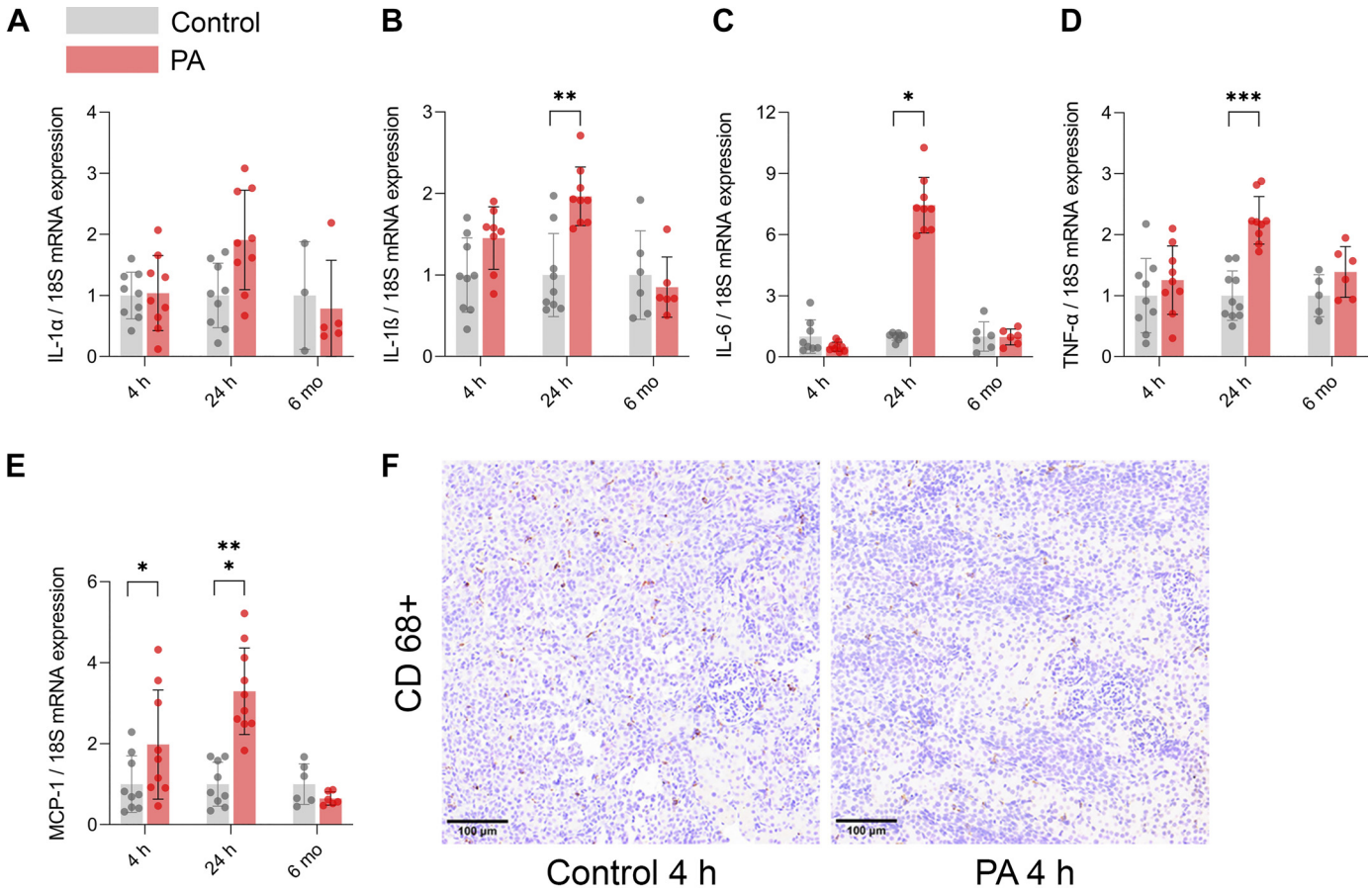

Figure 4. Perinatal asphyxia (PA) triggers proinflammatory processes in the kidney. *A–E*: renal mRNA expression of interleukin (IL)-1α (*Il1a*) (*A*), IL-1β (*Il1b*) (*B*), IL-6 (*Il6*) (*C*), tumor necrosis factor (TNF)-α (*Tnf*) (*D*), and monocyte chemoattractant protein (MCP)-1 (*Ccl2*) (*E*). Target gene expression levels were normalized to the 18S rRNA (*Rn18s*) housekeeping gene and presented as fold changes compared with controls. *F*: representative images of anti-CD68-labeled kidney tissue sections (×400 magnification, scale bar = 100 µm) to estimate macrophage infiltration. *P* values were determined by two-way ANOVA followed by Holm–Šídak's multiple-comparison (TNF-α and MCP-1) or Kruskal–Wallis test followed by Dunn's multiple comparison (IL-1α, IL-1β, and IL-6). $*P < 0.05$, $**P < 0.01$, and $***P < 0.001$ vs. control. $n = 3$–10/group. Gray bars represent the control group; red bars represent the PA group. Bars indicate means ± SD.

DISCUSSION

The severity of birth asphyxia is a major controversial topic among pediatricians. Neonates with mild encephalopathy are often excluded from therapeutic cooling practice. However, one should reckon with multiorgan consequences in their cases as well. Beyond the availability of effective treatment options, early recognition is crucial to mitigate long-term complications. Here we investigated various renal molecular pathways after PA to identify highly predictive renal parameters that may serve as biomarkers or targets for therapeutic development in the future.

The developmental stage at birth shows remarkable differences between species and organs. Thus, establishing a relevant preclinical model of birth asphyxia-related multiorgan damage is extremely difficult. Rats are physiologically born immature, and nephrogenesis is completed on *postnatal days 7–10* at the earliest (25). In contrast, in humans, nephrogenesis is completed during *gestational weeks 32–34* (26). Both species show reduced renal function and capacity during the first few postnatal weeks. In rats, these alterations are stabilized by *postnatal day 7*, resulting in similar resilience to hypoxic conditions as in human neonates. Considering all these, after fine tuning the model in pilot experiments, we believe our final setup using 7-day-old rats is a suitable model of kidney damage caused by PA.

Evaluation of kidney injury in neonates is challenging. Diagnostic relevance of the routinely used sCr is considered suboptimal in the early postnatal days (27) because it is biased by maternal levels (28) and is strongly modified by extrarenal factors, including muscle mass or protein intake (29). In addition, the half-life of creatinine is quite long; therefore, serum levels may take several days to reach a new steady-state value after glomerular filtration rate has changed. According to a recent clinical study, 20% of asphyxic neonates showed a delayed sCr response to injury, which makes it even less reliable as a biomarker (30).

The other classic renal retention parameter, BUN, was reported to be increased within the first 24 postnatal hours in neonates with asphyxia. In line with this, here we measured increased levels of BUN, indicating impaired renal function as an imminent consequence of PA. Conversely, others observed no BUN elevation in a different experimental PA

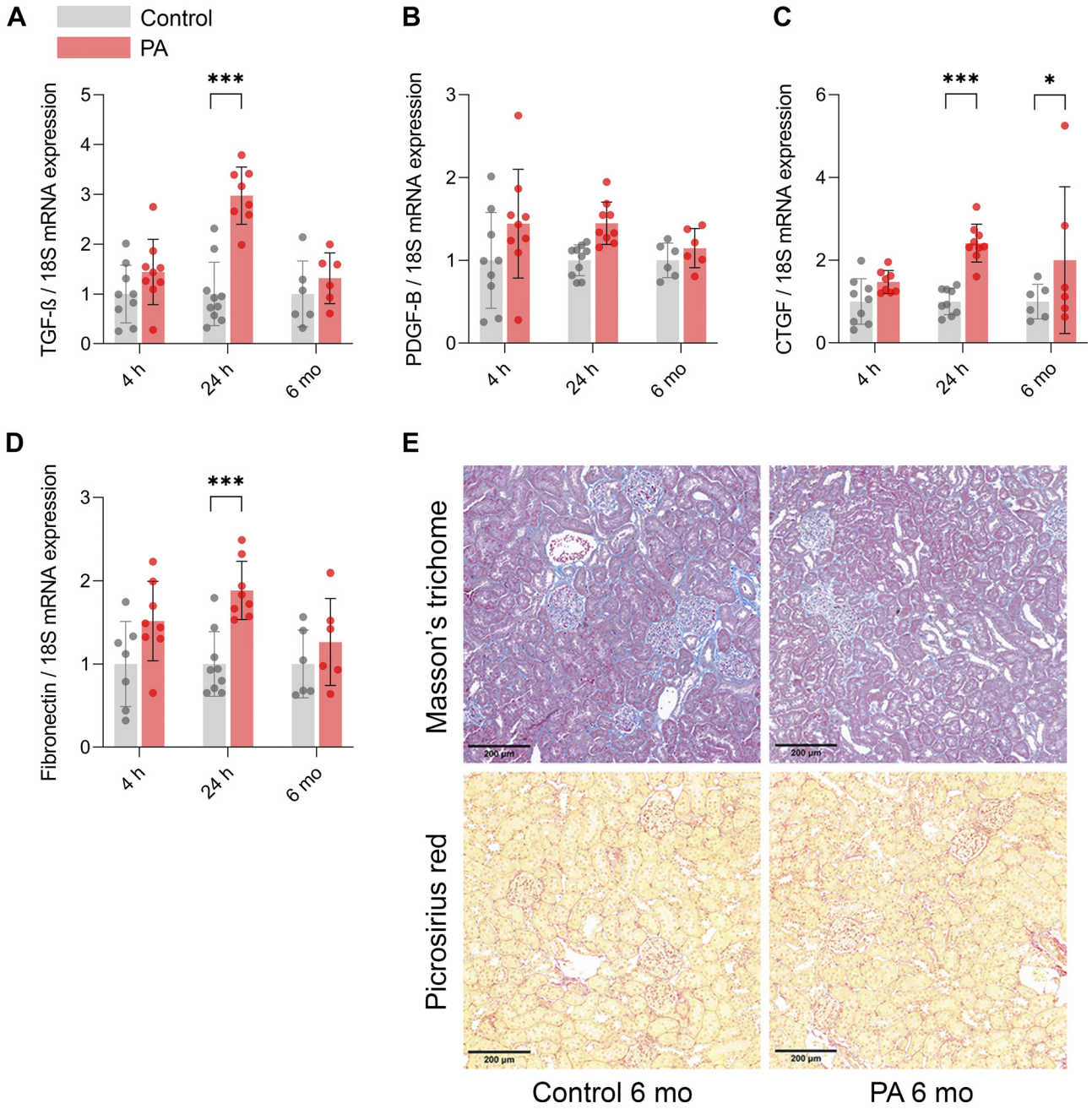

Figure 5. Perinatal asphyxia (PA) activates profibrotic mechanisms in the kidney. *A–D*: renal mRNA expression of transforming growth factor (TGF)-β (*Tgfb1*) (*A*), platelet-derived growth factor subunit B (PDGF-B; *Pdgfb*) (*B*), connective tissue growth factor (CTGF; *Ccn2*) (*C*), and fibronectin (*Fn1*) (*D*). Target gene expression levels were normalized to the 18S rRNA (*Rn18s*) housekeeping gene and presented as fold changes compared with controls. *E*: representative images of Masson's trichrome and picrosirius red-stained kidney tissue sections (×400 magnification; scale bar = 200 µm) of 6-mo-old rats to analyze interstitial fibrosis. *P* values were determined by two-way ANOVA followed by Holm–Šídak's multiple-comparison test. $^{*}P < 0.05$ and $^{***}P < 0.001$ vs. control. $n = 5$–10/group. Gray bars represent the control group; red bars represent PA group. Bars indicate means ± SD.

setup (31) (higher O_2: 4% vs. 8%, and longer time: 45 min vs. 2 h). They identified renal tubular dilation and shrinkage of glomeruli 24 h following the insult, which was not visible in our samples. Furthermore, these classic functional parameters are especially inadequate for the detection of subclinical AKI, and, therefore, the clinical "window of opportunity" for intervention may be missed (32). Thus, novel, more sensitive markers are desperately needed to improve diagnostic accuracy.

The utility of KIM-1 and NGAL as novel markers of kidney injury has been shown in numerous studies. In a pooled analysis of 10 studies of patients hospitalized in the intensive care unit, the authors showed that high NGAL levels were associated with poor outcomes even in the lack of diagnostic sCr elevations (33). In the clinical setting of PA, a multicenter prospective study found that urinary KIM-1 combined with birth weight outperformed sCr in diagnosing AKI. NGAL and IL-18 also had fair diagnostic performance at 24 h of life in

this study; moreover, the authors pointed out that a combination of these biomarkers may improve performance (21). Another study showed that serum KIM-1 is a good biomarker for the early detection of AKI in asphyxiated newborns (34). Congruently, we showed that PA leads to renal injury and upregulated KIM-1 and NGAL expression. Moreover, KIM-1 was elevated as early as 4 h after the insult, as a rapid indicator of proximal tubular damage. Our data suggest that KIM-1

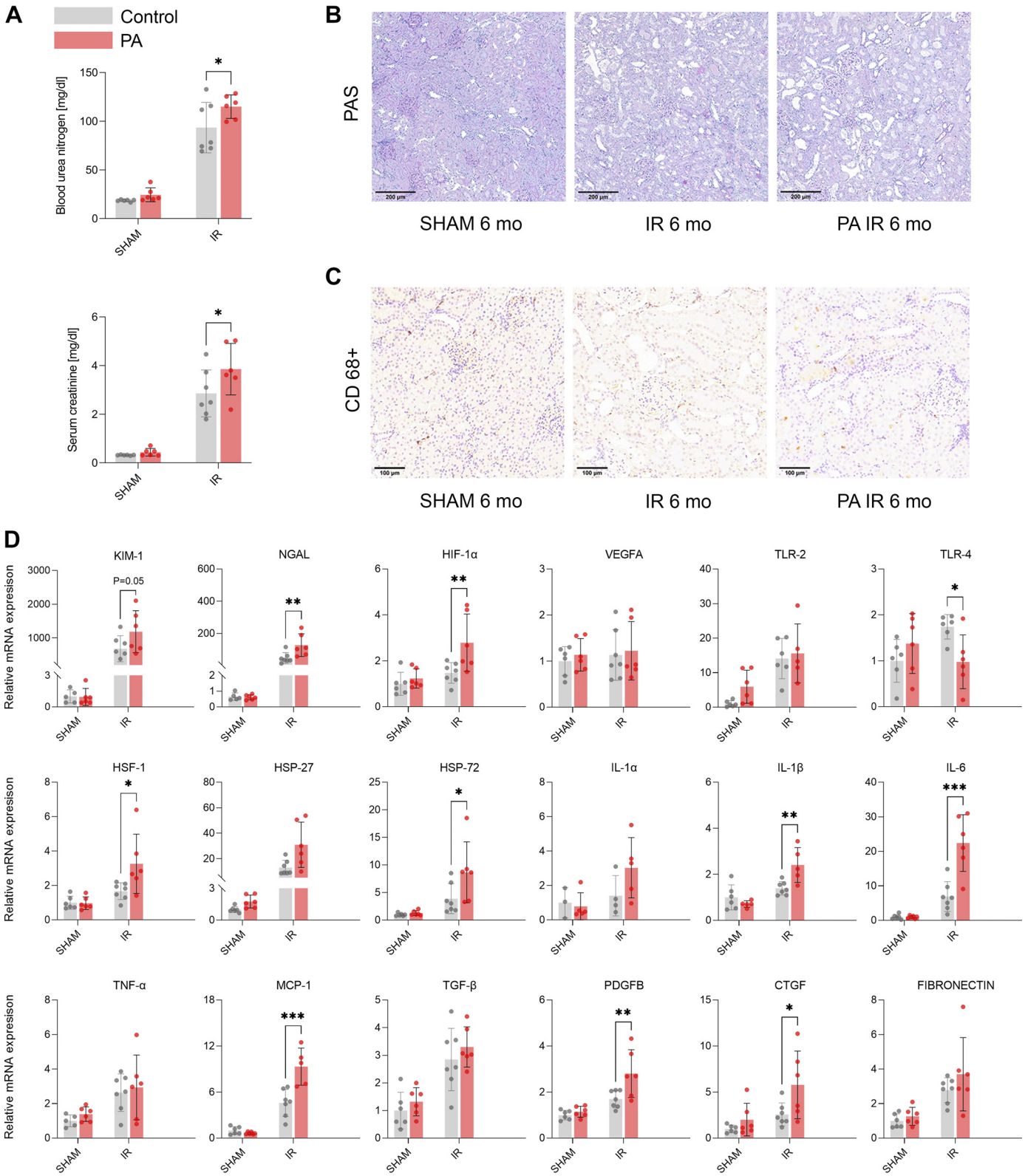

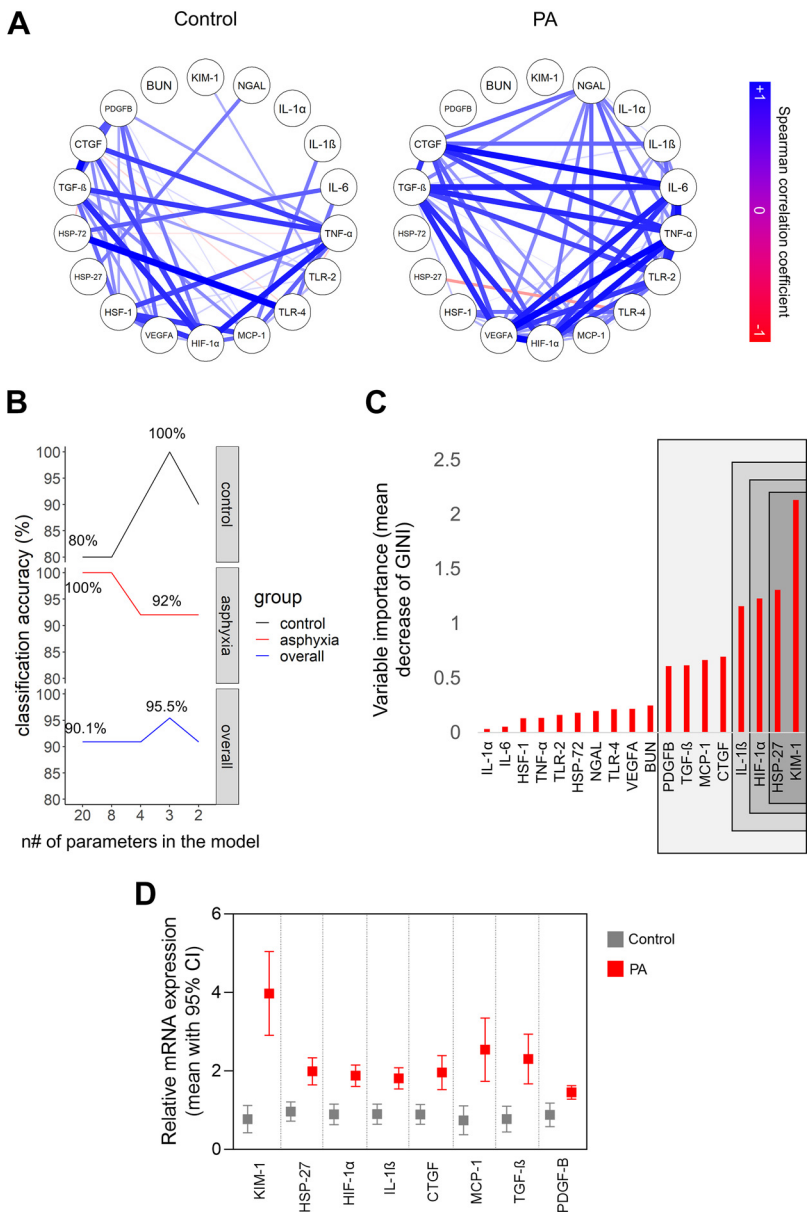

Figure 7. Random forest analysis provided subset models for the diagnosis of perinatal asphyxia (PA). *A*: network plot based on Spearman correlation analysis of measured features. Blue and red lines represent positive and negative correlations, respectively. The widths of the lines are proportional to the strength of the correlation. *B*: comparison of classification accuracy of the saturated model and the subset random forest model of different number of variables. Classification performance of the models is presented in each group individually and in the overall experimental population. Data values are presented in the saturated and the best performer subset models. *C*: variable importance plot based on Gini indices of variables. Gray rectangles enframe the set of variables of different subset models (8, 4, 3, and 2 variables). *D*: comparison of the eight most important variables in control and asphyxia groups. Bars indicate means with 95% confidence intervals. Diagrams present a subset of data that was used for the classification analysis.

and NGAL can be used as relevant markers of renal injury provoked by PA and may indicate subclinical AKI portending worse renal vulnerability later in life.

Hypoxic kidney injury initiates a complex cascade of molecular mechanisms that have not been studied systemically in relation to PA. Identifying association patterns between the activated pathways strongly contributes to a better understanding of PA's pathophysiological effects and the development of targeted therapies. Our measurements revealed a consistent upregulation of a broad range of genes associated with hypoxia, inflammation, angiogenesis, fibrosis, and the heat shock response. Moreover, cross-correlation analysis

Figure 6. Perinatal asphyxia (PA) permanently increases renal susceptibility to subsequent ischemia-reperfusion (IR) injury. *A*: serum levels of blood urea nitrogen and creatinine. *B*: representative images and of periodic acid-Schiff-stained kidney tissue sections (×400 magnification, scale bar = 200 μm) of 6-mo-old rats to analyze tubular lumen dilation. *C*: representative images of anti-CD68-labeled kidney tissue sections (×400 magnification, scale bar = 100 μm) to estimate macrophage infiltration. *D*: renal mRNA expression of kidney injury molecule (KIM)-1 (*Havcr1*), neutrophil gelatinase-associated lipocalin (NGAL; *Lcn2*), hypoxia-inducible factor (HIF)-1α (*Hif1a*), vascular endothelial growth factor A (VEGFA; *Vegfa*), Toll-like receptor (TLR)-2 (*Tlr2*), TLR-4 (*Tlr4*), heat shock factor (HSF)-1 (*Hsf1*), heat shock protein (HSP)-27 (*Hspb1*), HSP-72 (*Hspa2*), interleukin (IL)-1α (*Il1a*), IL-1β (*Il1b*), IL-6 (*Il6*), tumor necrosis factor (TNF)-α (*Tnf*), monocyte chemoattractant protein (MCP)-1 (*Ccl2*), transforming growth factor (TGF)-β (*Tgfb1*), platelet-derived growth factor subunit B (PDGF-B; *Pdgfb*), connective tissue growth factor (CTGF; *Ccn2*), and fibronectin (FIBRONECTIN; *Fn1*) in 6-mo-old rats. Target gene expression levels were normalized to the 18S rRNA (*Rn18s*) housekeeping gene and presented as fold changes compared with sham. *P* values were determined by two-way ANOVA followed by Holm–Šídak's multiple-comparison or Kruskal–Wallis test followed by Dunn's multiple comparison. $^{*}P < 0.05$, $^{**}P < 0.01$, and $^{***}P < 0.001$. $n = 5$–7/group. Bars indicate means ± SD.

identified emerging and collapsing correlations between the investigated genes and highlighted densely connected nodes that signify crucial variables.

Following PA, NGAL formed remarkable relationships with numerous immune mediators such as proinflammatory cytokines and chemokines (IL-6, TNF-α, and MCP-1), profibrotic factors (TGF-β and CTGF), and TLR-2. In addition, a correlation between NGAL, HIF-1α, and VEGFA mRNA expressions was observed. Inflammation is one of the main initiators of NGAL production (35, 36); however, the complexity of the association pattern revealed by our analysis suggests that multiple mechanisms influence its expression. Hypoxic response and inflammation are strongly interlinked processes; moreover, they have been demonstrated to regulate each other (37, 38). On the contrary, it has been shown that metabolic acidosis, an inevitable consequence of PA, directly regulates inflammatory processes (39). Although both mechanisms primarily support tissue regeneration and adaption to hypoxic conditions via the promotion of angiogenesis and tissue remodeling, prolonged or severe hypoxia together with unresolved inflammation may lead to post-AKI fibrosis and chronic renal dysfunction (40–43). We found that HIF-1α is a central node and therefore may be a key regulator of the pathomechanism of PA. However, further research is needed. Our results indicate that asphyxia promotes excessive inflammatory mediator production locally in the kidney, most likely by tubular epithelial cells and intrinsic immune cells, as we did not detect significant macrophage infiltration. The tubular epithelium is known to be actively involved in the inflammatory response to hypoxia by producing proinflammatory cytokines and chemokines as well as expressing TLRs, damage-associated molecular patterns, complement and complement receptors, and costimulatory molecules (44).

Interestingly, our statistical analysis did not show significant correlations between HSPs and other pathways; however, elevated mRNA expression of HSF-1 and HSP-27 clearly reflects the induction of heat shock response, which plays an important role in the protection against oxidative stress and the inhibition of renal fibrogenesis in renal ischemia (45, 46).

The diagnosis and prognosis of hypoxic-ischemic encephalopathy and multiorgan injury are low in sensitivity. Identifying novel biomarkers that can detect subclinical alterations would significantly advance neonatal care. Decision tree-based machine learning methods have become trending in the past decade and have been profitably implemented in various omics studies (47, 48). In the RF analysis, the subset model of three core variables (renal mRNA expressions of KIM-1, HIF-1α, and HSP-27) identified PA with an overall accuracy of 95.5%. Although this analysis is based on mRNA expression levels, KIM-1 and HSP-27 are routinely detected in serum in neonates with asphyxia (34, 49, 50). Moreover, although HIF-1α is not measured in serum, the routinely measured IL-1β is a similarly important parameter according to the Gini index. Interestingly, cross-correlation analysis identified HIF-1α as a key regulator; however, KIM-1 and HSP-27 showed no strong correlation with any other variable. These results indicate that delineation of the pathomechanism is necessary but not sufficient to select sensitive biomarkers.

Multiple studies have associated neonatal AKI with an increased risk of CKD later in life (51–53). Furthermore, even subclinical changes of kidney function are independently associated with progression to end-stage renal disease or a twofold risk of CKD (54–57). In line with this, although BUN and creatinine clearance values did not change in adult rats, HSP-27, TLR-2, and CTGF expressions persistently increased, pointing to possible permanent, subclinical effects of PA. This hypothesis was tested on healthy and post-PA rats subjected to renal IR at 6 mo. Indeed, post-PA adult rats suffered more severe functional decline and tubular injury after renal IR. Furthermore, hypoxic, heat shock, inflammatory, and profibrotic pathways were more robustly activated in PA IR rats than controls. These results suggest that PA may provoke a dysregulated molecular environment with inflammatory reprogramming early in life, which mounts up to increased sensitivity to subsequent insults. It should be noted that repeated exposure to mild hypoxia can confer protection against subsequent AKI (58–60). However, the conditions we used to mimic PA are different from those typically used for hypoxic preconditioning: single exposure with lower O_2 levels and high CO_2 levels, which model the basic and relevant features of PA, i.e., hypoxia with respiratory acidosis (13, 14). There are extensive data showing that the basic features of PA (hypoxia with respiratory acidosis) are not mimicked in animal models based on hypoxia only (13, 14). In addition, immature kidneys are especially susceptible to hypoxic injury, underscoring the need for further investigations to validate the effects of hypoxia at this developmental stage. Nevertheless, the current findings highlight the importance of both the severity and frequency of hypoxic exposure in determining the outcome.

Taken together, PA activated major molecular pathways in the kidney, which resulted in subclinical tubular injury. RF analysis revealed an outstanding predictive value of our trinomial model, which is a potential basis for further PA biomarker research. Our findings clearly demonstrate that PA may have lifelong consequences regarding the kidney and may be a risk factor for diseases with renal involvement. From the clinical aspect, regular checkups of kidney function and extra precautions during particular interventions (e.g., imaging with contrast media, supra-aortic surgeries) are worth considering in the PA-affected and preterm population.

DATA AVAILABILITY

Data supporting the findings of this study are available within the article. Primer sequences and summary statistics are publicly available in Supplemental Table S1 and Supplemental Table S2, respectively.

SUPPLEMENTAL MATERIAL

Supplemental Fig. S1 and Supplemental Tables S1 and S2: https://doi.org/10.6084/m9.figshare.25886536.v2.

ACKNOWLEDGMENTS

The authors thank Aron Kerenyi, Eszter Sipos, Ganna Stepanova, Agnes Molnar, and Csaba Nador for the excellent technical help and intellectual contributions.

GRANTS

This work was funded by the following grants: Hungarian Scientific Research Fund (PD131637, K135398, K135292, and PC2022-8/2022); Project No. TKP2021-EGA-24 has been implemented with support from the Ministry of Innovation and Technology of Hungary from the National Research, Development and Innovation Fund, financed under the TKP2021-EGA (Thematic Excellence Programme 2021-Health Subprogramme) funding scheme, and was also supported by MTA-SE "Lendület" Research Grant LP2021-3/2021 and National Laboratory Grant RRF-2.3.1-21-2022-00011; National Research, Development and Innovation Fund, Ministry of Innovation and Technology of Hungary: PD131637 (to A.H.), K135398 (to A.F.), K135292 (to E.M.), TKP2021-EGA-24 (to A.F.), and RRF-2.3.1-21-2022-00011 (to E.M.), and Hungarian Academy of Sciences: PC2022-8/2022 (to A.F.) and LP2021-3/2021 (to A.F.).

DISCLOSURES

No conflicts of interest, financial or otherwise, are declared by the authors.

AUTHOR CONTRIBUTIONS

A.F., K.D., M.S., K.K., A.D., E.M., and A.H. conceived and designed research; T.L., K.D., A.R.T., H.K., and A.B. performed experiments; T.L., Z.K.V., A.P., and A.B. analyzed data; T.L., A.F., Z.K.V., A.P., M.S., K.K., A.D., E.M., and A.H. interpreted results of experiments; T.L. and Z.K.V. prepared figures; T.L., A.F., Z.K.V., M.S., and E.M. drafted manuscript; T.L., A.F., K.D., K.K., A.D., E.M., and A.H. edited and revised manuscript; A.F., M.S., A.J.S., K.K., A.D., E.M., and A.H. approved final version of manuscript.

REFERENCES

1. **World Health Organization.** *Perinatal Asphyxia* [Online]. https://www.who.int/teams/maternal-newborn-child-adolescent-health-and-ageing/newborn-health/perinatal-asphyxia.
2. **Graham EM**, **Ruis KA**, **Hartman AL**, **Northington FJ**, **Fox HE.** A systematic review of the role of intrapartum hypoxia-ischemia in the causation of neonatal encephalopathy. *Am J Obstet Gynecol* 199: 587–595, 2008. doi:10.1016/J.AJOG.2008.06.094.
3. **Lee ACC**, **Kozuki N**, **Blencowe H**, **Vos T**, **Bahalim A**, **Darmstadt GL**, **Niermeyer S**, **Ellis M**, **Robertson NJ**, **Cousens S**, **Lawn JE.** Intrapartum-related neonatal encephalopathy incidence and impairment at regional and global levels for 2010 with trends from 1990. *Pediatr Res* 74, *Suppl* 1: 50–72, 2013. doi:10.1038/pr.2013.206.
4. **Natarajan G**, **Pappas A**, **Shankaran S.** Outcomes in childhood following therapeutic hypothermia for neonatal hypoxic-ischemic encephalopathy (HIE). *Semin Perinatol* 40: 549–555, 2016. doi:10.1053/J.SEMPERI.2016.09.007.
5. **O'Dea M**, **Sweetman D**, **Bonifacio SL**, **El-Dib M**, **Austin T**, **Molloy EJ.** Management of multi organ dysfunction in neonatal encephalopathy. *Front Pediatr* 8: 239, 2020. doi:10.3389/FPED.2020.00239.
6. **Larosa DA**, **Ellery SJ**, **Walker DW**, **Dickinson H.** Understanding the full spectrum of organ injury following intrapartum asphyxia. *Front Pediatr* 5: 16, 2017. doi:10.3389/fped.2017.00016.
7. **Iribarren I**, **Hilario E**, **Álvarez A**, **Alonso-Alconada D.** Neonatal multiple organ failure after perinatal asphyxia. *An Pediatr (Engl Ed)* 97: 280.e1–280.e8, 2022. doi:10.1016/j.anpede.2022.08.010.
8. **Askenazi DJ**, **Feig DI**, **Graham NM**, **Hui-Stickle S**, **Goldstein SL.** 3-5 year longitudinal follow-up of pediatric patients after acute renal failure. *Kidney Int* 69: 184–189, 2006. doi:10.1038/SJ.KI.5000032.
9. **Chock VY**, **Frymoyer A**, **Yeh CG**, **Van Meurs KP.** Renal saturation and acute kidney injury in neonates with hypoxic ischemic encephalopathy undergoing therapeutic hypothermia. *J Pediatr* 200: 232–239.e1, 2018. doi:10.1016/J.JPEDS.2018.04.076.
10. **Ronco C**, **Kellum JA**, **Haase M.** Subclinical AKI is still AKI. *Crit Care* 16: 313–314, 2012. doi:10.1186/CC11240/TABLES/1.
11. **Nickolas TL**, **Schmidt-Ott KM**, **Canetta P**, **Forster C**, **Singer E**, **Sise M**, **Elger A**, **Maarouf O**, **Sola-Del Valle DA**, **O'Rourke M**, **Sherman E**, **Lee P**, **Geara A**, **Imus P**, **Guddati A**, **Polland A**, **Rahman W**, **Elitok S**, **Malik N**, **Giglio J**, **El-Sayegh S**, **Devarajan P**, **Hebbar S**, **Saggi SJ**, **Hahn B**, **Kettritz R**, **Luft FC**, **Barasch J.** Diagnostic and prognostic stratification in the emergency department using urinary biomarkers of nephron damage: a multicenter prospective cohort study. *J Am Coll Cardiol* 59: 246–255, 2012. doi:10.1016/J.JACC.2011.10.854.
12. **Marcello M**, **Virzì GM**, **Muciño-Bermejo M-J**, **Manani SM**, **Giavarina D**, **Salvador L**, **Ronco C**, **Zanella M.** Subclinical AKI and clinical outcomes in elderly patients undergoing cardiac surgery: diagnostic utility of NGAL versus standard creatinine increase criteria. *Cardiorenal Med* 12: 94–105, 2022. doi:10.1159/000525221.
13. **Pospelov AS**, **Puskarjov M**, **Kaila K**, **Voipio J.** Endogenous brain-sparing responses in brain pH and PO_2 in a rodent model of birth asphyxia. *Acta Physiol (Oxf)* 229: e13467, 2020. doi:10.1111/APHA.13467.
14. **Summanen M**, **Bäck S**, **Voipio J**, **Kaila K.** Surge of peripheral arginine vasopressin in a rat model of birth asphyxia. *Front Cell Neurosci* 12: 2, 2018. doi:10.3389/FNCEL.2018.00002.
15. **Wen Z**, **Luo D**, **Wang S**, **Rong R**, **Evers BM**, **Jia L**, **Fang Y**, **Daoud EV**, **Yang S**, **Gu Z**, **Arner EN**, **Lewis CM**, **Solis Soto LM**, **Fujimoto J**, **Behrens C**, **Wistuba II**, **Yang DM**, **Brekken RA**, **O'Donnell KA**, **Xie Y**, **Xiao G.** Deep learning–based H-score quantification of immunohistochemistry-stained images. *Mod Pathol* 37: 100398, 2024. doi:10.1016/J.MODPAT.2023.100398.
16. **Breiman L.** Random forests. *Mach Learn* 45: 5–32, 2001. doi:10.1023/A:1010933404324.
17. **Epskamp S**, **Cramer AOJ**, **Waldorp LJ**, **Schmittmann VD**, **Borsboom D.** qgraph: network visualizations of relationships in psychometric data. *J Stat Soft* 48: 1–18, 2012. doi:10.18637/JSS.V048.I04.
18. **Liaw A**, **Wiener M.** *Classification and Regression by randomForest* [Online]. https://journal.r-project.org/articles/RN-2002-022/RN-2002-022.pdf [Accessed 6 October 2022].
19. **Genuer R**, **Poggi J-M**, **Tuleau-Malot C.** *VSURF: an R Package for Variable Selection Using Random Forests* [Online]. http://cran.r-project.org/package=VSURF [Accessed 6 October 2022].
20. **R Core Team.** *R: a Language and Environment for Statistical Computing* [Online]. Vienna, Austria: R Foundation for Statistical Computing, 2022. https://www.r-project.org/.
21. **Rumpel J**, **Spray BJ**, **Chock VY**, **Kirkley MJ**, **Slagle CL**, **Frymoyer A**, **Cho SH**, **Gist KM**, **Blaszak R**, **Poindexter B**, **Courtney SE.** Urine biomarkers for the assessment of acute kidney injury in neonates with hypoxic ischemic encephalopathy receiving therapeutic hypothermia. *J Pediatr* 241: 133–140.e3, 2022. doi:10.1016/J.JPEDS.2021.08.090.
22. **Shu S**, **Wang Y**, **Zheng M**, **Liu Z**, **Cai J**, **Tang C**, **Dong Z.** Hypoxia and hypoxia-inducible factors in kidney injury and repair. *Cells* 8: 207, 2019. doi:10.3390/CELLS8030207.
23. **Chen H**, **Liu N**, **Zhuang S.** Macrophages in renal injury, repair, fibrosis following acute kidney injury and targeted therapy. *Front Immunol* 13: 934299, 2022. doi:10.3389/FIMMU.2022.934299.
24. **Black LM**, **Lever JM**, **Agarwal A.** Renal inflammation and fibrosis: a double-edged sword. *J Histochem Cytochem* 67: 663–681, 2019. doi:10.1369/0022155419852932.
25. **Maric C**, **Ryan GB**, **Alcorn D.** Embryonic and postnatal development of the rat renal interstitium. *Anat Embryol (Berl)* 195: 503–514, 1997. doi:10.1007/S004290050070.
26. **Rookmaaker MB**, **Joles JA.** The nephron number counts–from womb to tomb. *Nephrol Dial Transplant* 28: 1325–1328, 2013. doi:10.1093/NDT/GFS538.
27. **Edelstein CL.** Biomarkers of acute kidney injury. *Adv Chronic Kidney Dis* 15: 222–234, 2008. doi:10.1053/J.ACKD.2008.04.003.
28. **Go H**, **Momoi N**, **Kashiwabara N**, **Haneda K**, **Chishiki M**, **Imamura T**, **Sato M**, **Goto A**, **Kawasaki Y**, **Hosoya M.** Neonatal and maternal serum creatinine levels during the early postnatal period in preterm and term infants. *PLoS One* 13: e0196721, 2018. doi:10.1371/JOURNAL.PONE.0196721.
29. **Delanaye P**, **Cavalier E**, **Pottel H.** Serum creatinine: not so simple! *Nephron* 136: 302–308, 2017. doi:10.1159/000469669.
30. **Gupta C**, **Massaro AN**, **Ray PE.** A new approach to define acute kidney injury in term newborns with hypoxic ischemic encephalopathy. *Pediatr Nephrol* 31: 1167–1178, 2016. doi:10.1007/S00467-016-3317-5.
31. **Plotnikov EY**, **Pavlenko TA**, **Pevzner IB**, **Zorova LD**, **Manskikh VN**, **Silachev DN**, **Sukhikh GT**, **Zorov DB.** The role of oxidative stress in

acute renal injury of newborn rats exposed to hypoxia and endotoxin. *FEBS J* 284: 3069–3078, 2017. doi:10.1111/FEBS.14177.

32. **Schrezenmeier EV**, **Barasch J**, **Budde K**, **Westhoff T**, **Schmidt-Ott KM.** Biomarkers in acute kidney injury – pathophysiological basis and clinical performance. *Acta Physiol (Oxf)* 219: 554–572, 2017. doi:10.1111/APHA.12764.
33. **Haase M**, **Devarajan P**, **Haase-Fielitz A**, **Bellomo R**, **Cruz DN**, **Wagener G**, **Krawczeski CD**, **Koyner JL**, **Murray P**, **Zappitelli M**, **Goldstein SL**, **Makris K**, **Ronco C**, **Martensson J**, **Martling CR**, **Venge P**, **Siew E**, **Ware LB**, **Ikizler TA**, **Mertens PR.** The outcome of neutrophil gelatinase-associated lipocalin-positive subclinical acute kidney injury: a multicenter pooled analysis of prospective studies. *J Am Coll Cardiol* 57: 1752–1761, 2011. doi:10.1016/J.JACC.2010.11.051.
34. **Mehrkesh M**, **Barekatain B**, **Gheisari A**, **Ahmadi M**, **Shahsanai A.** Serum KIM-1 and cystatin levels as the predictors of acute kidney injury in asphyxiated neonates. *Iran J Neonatol* 13: 6–12, 2022. doi:10.22038/IJN.2021.58428.2126.
35. **Bonnemaison ML**, **Marks ES**, **Boesen EI.** Interleukin-1β as a driver of renal NGAL production. *Cytokine* 91: 38–43, 2017. doi:10.1016/J.CYTO.2016.12.004.
36. **Chakraborty S**, **Kaur S**, **Guha S**, **Batra SK.** The multifaceted roles of neutrophil gelatinase associated lipocalin (NGAL) in inflammation and cancer. *Biochim Biophys Acta* 1826: 129–169, 2012. doi:10.1016/J.BBCAN.2012.03.008.
37. **Haase VH.** Inflammation and hypoxia in the kidney: friends or foes? *Kidney Int* 88: 213–215, 2015. doi:10.1038/KI.2015.89.
38. **Li ZL**, **Ji JL**, **Wen Y**, **Cao JY**, **Kharbuja N**, **Ni WJ**, **Yin D**, **Feng ST**, **Liu H**, **Lv LL**, **Liu BC**, **Wang B.** HIF-1α is transcriptionally regulated by NF-κB in acute kidney injury. *Am J Physiol Renal Physiol* 321: F225–F235, 2021. doi:10.1152/AJPRENAL.00119.2021.
39. **Hudalla H**, **Michael Z**, **Christodoulou N**, **Willis GR**, **Fernandez-Gonzalez A**, **Filatava EJ**, **Dieffenbach P**, **Fredenburgh LE**, **Stearman RS**, **Geraci MW**, **Kourembanas S**, **Christou H.** Carbonic anhydrase inhibition ameliorates inflammation and experimental pulmonary hypertension. *Am J Respir Cell Mol Biol* 61: 512–524, 2019. doi:10.1165/RCMB.2018-0232OC.
40. **Higgins DF**, **Biju MP**, **Akai Y**, **Wutz A**, **Johnson RS**, **Haase VH.** Hypoxic induction of *Ctgf* is directly mediated by Hif-1. *Am J Physiol Renal Physiol* 287: F1223–F1232, 2004. doi:10.1152/ajprenal.00245.2004.
41. **Medzhitov R.** Inflammation 2010: new adventures of an old flame. *Cell* 140: 771–776, 2010. doi:10.1016/J.CELL.2010.03.006.
42. **Kurts C**, **Panzer U**, **Anders HJ**, **Rees AJ.** The immune system and kidney disease: basic concepts and clinical implications. *Nat Rev Immunol* 13: 738–753, 2013. doi:10.1038/NRI3523.
43. **Anders HJ**, **Schaefer L.** Beyond tissue injury-damage-associated molecular patterns, toll-like receptors, and inflammasomes also drive regeneration and fibrosis. *J Am Soc Nephrol* 25: 1387–1400, 2014. doi:10.1681/ASN.2014010117.
44. **Bonventre JV**, **Yang L.** Cellular pathophysiology of ischemic acute kidney injury. *J Clin Invest* 121: 4210–4221, 2011. doi:10.1172/JCI45161.
45. **Mehlen P**, **Hickey E**, **Weber LA**, **Arrigo AP.** Large unphosphorylated aggregates as the active form of hsp27 which controls intracellular reactive oxygen species and glutathione levels and generates a protection against TNFα in NIH-3T3-ras cells. *Biochem Biophys Res Commun* 241: 187–192, 1997. doi:10.1006/BBRC.1997.7635.
46. **Vidyasagar A**, **Reese SR**, **Hafez O**, **Huang LJ**, **Swain WF**, **Jacobson LM**, **Torrealba JR**, **Chammas PE**, **Wilson NA**, **Djamali A.** Tubular expression of heat-shock protein 27 inhibits fibrogenesis in obstructive nephropathy. *Kidney Int* 83: 84–92, 2013. doi:10.1038/KI.2012.336.
47. **Acharjee A**, **Kloosterman B**, **de Vos RCH**, **Werij JS**, **Bachem CWB**, **Visser RGF**, **Maliepaard C.** Data integration and network reconstruction with ~omics data using Random Forest regression in potato. *Anal Chim Acta* 705: 56–63, 2011. doi:10.1016/J.ACA.2011.03.050.
48. **Degenhardt F**, **Seifert S**, **Szymczak S.** Evaluation of variable selection methods for random forests and omics data sets. *Brief Bioinform* 20: 492–503, 2019. doi:10.1093/bib/bbx124.
49. **Farhat A**, **Shafiee M**, **Mohammadzadeh A**, **Saeidi R**, **Amiri R**, **Ghayour-Mobarhan M.** Association of neonatal asphyxia with serum levels of heat shock protein 27 in a small sample of newborns. *Acta Med Iran* 57: 303–307, 2019. doi:10.18502/ACTA.V57I5.1866.
50. **Cao XY**, **Zhang HR**, **Zhang W**, **Chen B.** [Diagnostic values of urinary netrin-1 and kidney injury molecule-1 for acute kidney injury induced by neonatal asphyxia]. *Zhongguo Dang Dai Er Ke Za Zhi* 18: 24–28, 2016. doi:10.7499/J.ISSN.1008-8830.2016.01.006.
51. **Alkandari O**, **Eddington KA**, **Hyder A**, **Gauvin F**, **Ducruet T**, **Gottesman R**, **Phan V**, **Zappitelli M.** Acute kidney injury is an independent risk factor for pediatric intensive care unit mortality, longer length of stay and prolonged mechanical ventilation in critically ill children: a two-center retrospective cohort study. *Crit Care* 15: R146–12, 2011. doi:10.1186/cc10269.
52. **Polito C**, **Papale MR**, **La Manna A.** Long-term prognosis of acute renal failure in the full-term neonate. *Clin Pediatr (Phila)* 37: 381–385, 1998. doi:10.1177/000992289803700609.
53. **Carmody JB**, **Charlton JR.** Short-term gestation, long-term risk: prematurity and chronic kidney disease. *Pediatrics* 131: 1168–1179, 2013. doi:10.1542/PEDS.2013-0009.
54. **Liotta M**, **Olsson D**, **Sartipy U**, **Holzmann MJ.** Minimal changes in postoperative creatinine values and early and late mortality and cardiovascular events after coronary artery bypass grafting. *Am J Cardiol* 113: 70–75, 2014. doi:10.1016/J.AMJCARD.2013.09.012.
55. **Lassnigg A**, **Schmid ER**, **Hiesmayr M**, **Falk C**, **Druml W**, **Bauer P**, **Schmidlin D.** Impact of minimal increases in serum creatinine on outcome in patients after cardiothoracic surgery: do we have to revise current definitions of acute renal failure? *Crit Care Med* 36: 1129–1137, 2008. doi:10.1097/CCM.0B013E318169181A.
56. **Newsome BB**, **Warnock DG**, **McClellan WM**, **Herzog CA**, **Kiefe CI**, **Eggers PW**, **Allison JJ.** Long-term risk of mortality and end-stage renal disease among the elderly after small increases in serum creatinine level during hospitalization for acute myocardial infarction. *Arch Intern Med* 168: 609–616, 2008. doi:10.1001/ARCHINTE.168.6.609.
57. **Ishani A**, **Nelson D**, **Clothier B**, **Schult T**, **Nugent S**, **Greer N**, **Slinin Y**, **Ensrud KE.** The magnitude of acute serum creatinine increase after cardiac surgery and the risk of chronic kidney disease, progression of kidney disease, and death. *Arch Intern Med* 171: 226–233, 2011 [Erratum in *Arch Intern Med* 171: 1919, 2011]. doi:10.1001/ARCHINTERNMED.2010.514.
58. **Späth MR**, **Bartram MP**, **Palacio-Escat N**, **Hoyer KJR**, **Debes C**, **Demir F**, **Schroeter CB**, **Mandel AM**, **Grundmann F**, **Ciarimboli G**, **Beyer A**, **Kizhakkedathu JN**, **Brodesser S**, **Göbel H**, **Becker JU**, **Benzing T**, **Schermer B**, **Höhne M**, **Burst V**, **Saez-Rodriguez J**, **Huesgen PF**, **Müller RU**, **Rinschen MM.** The proteome microenvironment determines the protective effect of preconditioning in cisplatin-induced acute kidney injury. *Kidney Int* 95: 333–349, 2019. doi:10.1016/J.KINT.2018.08.037.
59. **Yang CC**, **Lin LC**, **Wu MS**, **Chien CT**, **Lai MK.** Repetitive hypoxic preconditioning attenuates renal ischemia/reperfusion induced oxidative injury via upregulating HIF-1α-dependent bcl-2 signaling. *Transplantation* 88: 1251–1260, 2009. doi:10.1097/TP.0B013E3181BB4A07.
60. **Bernhardt WM**, **Câmpean V**, **Kany S**, **Jürgensen JS**, **Weidemann A**, **Warnecke C**, **Arend M**, **Klaus S**, **Günzler V**, **Amann K**, **Willam G**, **Wiesener MS**, **Eckardt KU.** Preconditional activation of hypoxia-inducible factors ameliorates ischemic acute renal failure. *J Am Soc Nephrol* 17: 1970–1978, 2006. doi:10.1681/ASN.2005121302.